

Simulation and Investigation of Solar based BLDC Motor Drives for High Speed Surgical Hand Tools Application

¹Veeramuthulingam Nagarajan, ²Ezhilarasi Arivukkannu, ³Ramaswamy Muthiah

¹Research Scholar, ²Associate Professor, ³Professor

^{1,2,3}Department of Electrical Engineering, Annamalai University, Annamalai Nagar, Tamil Nadu, India.
sethukumark@gmail.com

Article Info

Volume 83

Page Number: 1311 - 1321

Publication Issue:

March - April 2020

Abstract

The paper approached model reference adaptive control for best the performance of solar environment fed Brushless dc motor. The emphasis orients to model the motor in the steady state framework and intrigues the theory of model reference adaptive principles for reaching out to address the performance improvement. It offers with the use of a dc to dc converter in solar environment primarily based as a transitional DC-DC converter between a photo voltaic array and a Five Level inverter to achieve the most excessive power of the photo voltaic array and as a consequence the subtle begin of the brushless motor drives by appropriate regulation. A variable dc link voltage acting as controller is completed by the converter which is used as a front-end converter. It's consisting of single semiconductor switch and less number components, buck boost converter displays awesome change effectiveness. This only one converter structure permitting follows- up of solar environment maximum power point tracking (MPPT) regardless of irradiance and temperature. The acquired from the solar array exhibit the perturb & Observe tracking techniques by process. For decreased wide variety of switches employing BLDC Drive, this multilevel inverter topology is proposed. The current work focuses on improving BLDC drives output than when applied with ordinary inverters, and using staggered inverters. The dynamic and stable performance of the proposal through the use of the Simulink condition MatLab tool compartments.

Article History

Article Received: 24 July 2019

Revised: 12 September 2019

Accepted: 15 February 2020

Publication: 14 March 2020

Keywords: PV Array, Multilevel Inverter (NPC), Buck-Boost converter BLDC, Model Reference Adaptive Control

1. Introduction

A sustained reduction in the cost of photovoltaic panels and electronic power units has allowed industries and researchers to use the energy generated through the photovoltaic array for separate applications. A Solar energy is one of renewable energy's highest common and fastest-growing energy. PV panels in the modern years and their prolonged life have extended photovoltaic (PV)-based era two for a separate household, automatic irrigation system with the assistance of motor drives, choppers, and industry. Though various researches have been carried out on PV array fed automotive and

irrigation structures combining quite a number DC-DC converters and control of motor drives. A most effectivity of the photovoltaic array is a maximum power point tracking (MPPT) approach to converter use over the entire executed via. Specific DC-DC converters, such as Boost[1], buck boost[2], buck[3], have been used for MPPT in real world applications based on special photo voltaic arrays.

Choosing Maximum Power Point Tracking and DC-DC converter is crucial for the most efficient overall performance of the primarily water pumping application based on solar energy. There are two very important

MPPT techniques in this research, such as Incremental Conductance (INC), and Perturb & Observe (P&O). Perturb & Observe is very robust, modest, accessible to manage but its efficiency under varying ecological conditions is depreciated by the problems with the P&O [4]. The Buck-Boost converter is ideal for solar-based water pumping applications; it can be worked in both boost mode and buck mode in unrestrained working region in conjunction with Gate pulse (Duty cycle) [5]. BLDC motor drives are used in a wide range of industrial and home applications due to numerous performance evidence such as simple structure, high efficiency, high power factor, high power density, quick dynamic response, high torque starting rate, high speed range, low acoustic noise and easy handling due to linear voltage speed and torque to current [6].

Open-loop control methods are used in motor manipulation applications to adjust the motor speed by directly controlling the PWM signal and running the motor drive circuit. The PWM pulse duty cycle controls the switch ON of the motor-drive circuit in IGBTs and this in turn regulates the specific voltage supplied throughout the motor's armature. In a closed loop control system, the output state has a direct effect on the condition of the input. In this approach speed is controlled in a closed loop by authentic motor speed calculation. The error is premeditated in fixed speed and variable speed. Using a PI controller, the speed error is increased and the PWM gate pulse duty cycle dynamically regulated [7].

With the help of a dc-dc converter, the power extracted from the photo voltaic array is regulated to the appropriate dc voltage. The motor used to power either DC or AC motors for pumping applications. The DC motors can be quickly attached to the photo voltaic array. Thus the stage of adaptation can be sidestepped. Yet DC motors have the downside of constant brushes put on and tear and wide-ranging maintenance. The Induction motors require complicated handling and are therefore no longer preferred additionally [8].

The Karnaugh map is usable, in addition dynamic speed management strategy is introduced, Karnaugh map is its dynamic speed control for very simple fixed load, now a day of precise speed controls and very complex and is also available but this manipulation is very easy and important for any form of multilevel inverter, so this control is limited to THD on the utility side, in this project. In addition, in this mission precision, the range of the inverter stage can be increased so that the amount of pulses can also be increased through Karnaugh map logic, two of which are additionally beneficial for electronically switched multiphase motors [9].

In contrast to traditional topology, the modified multilevel inverter structure uses only nine switches and a diode which reduces semi-conductor switching losses and cost. Simulation tests annotations of the regenerative braking strategy, distinctive braking systems are extra beneficial in terms of switching length and recovery of

electricity. But regenerative braking approach is really costly, as some external circuitry is required. It is advised to use dynamic braking strategy where the braking has greater importance than the energy to be lost. While plugging offers faster braking retort, this method is inefficient when you realize that a huge amount of braking resistance is wasted [10].

Another suggested approach Once calculated by a voltage source inverter, engine output is equated with BLDC motor once regulated by the use of five level H bridge inverter with stage shifted SPWM MLI for similar motor constraints. As the voltage stages will minimize THD production, torque ripples low [11].

A speed estimation control calculation was created utilizing the MRAC standards without the need to change the engine parameters and requires the utilization of fast back emf coefficient and low speed stator resistors [12]-[14]. Versatile Neuro Fluffy surmising framework (ANFIS) that depends on control the BLDC engine. It's the guideline of speed that that is diminished by rise time and setting time. The principle bit of leeway of the present calculation depends on supervisory learning calculation is presented. This strategy is pondered in such a manner to startup power, control the torque and furthermore for improving the dynamic execution of the framework [15].

The paper is sorted out as follows: The idea of framework design is clarified in area II. The displaying of a photovoltaic and MPPT algorithm is discussed about in segment III. The multilevel inverter fed BLDC engine is detailed in area IV. The Simulation results are examined in segment V. At last, the Conclusion in area VII.

2. Proposed System Formation

Figure 1 showed the shape of the proposed buck boost converter based on photo voltaic fed Brushless motor drives for surgical hand tools. The proposed gadget includes five level NPC inverter, photo voltaic, buck boost converter, BLDC motor and hand tool set for surgical operation. Solar power is monitored using the photo voltaic array which maintains efficiency through the MPPT system. With the help of techniques for a dc-dc converter, the unregulated dc voltage at the PV system yield is determined by a controlled dc voltage. Within the converter the duty ratio of a switch is controlled via the MPPT method. The inverter pulses for the Gate are generated using a truth table using back-emf.

3. Design of the Solar and MPPT Algorithm

The different operating stages of the configuration displayed in the figure1, such as the PV array, Buck Boost converter, load design such that a satisfactory operation always accomplished.

It converts sun light intensity to electrical energy, the main component of the solar PV array is solar cells, which are constructed with P-N junction photodiodes with broad sensitive area of light. An individual solar cell

unit's equivalent circuit replicates a current source in parallel to an internal diode, as shown in Fig 2. The current source production is directly proportional to the luminous intensity on the cell.

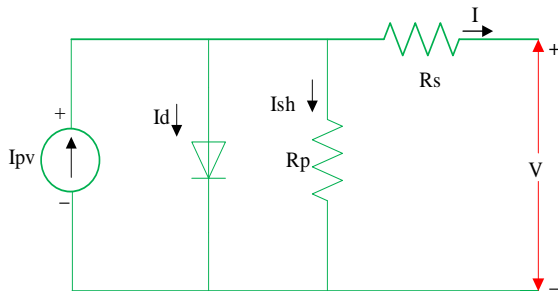


Figure 2: Practical PV cell model

Solar power is 1000 W capacity the limitations of the PV array are predictable in the 1000 W / m² photovoltaic insolation stage and 25°C temperature. A PV module is built by connecting 72 photovoltaic PV cells in collection which reaches its maximum power at 77% of open circuit voltage and 90% of short circuit current.

PV array at Maximum Power Point is nominated in view of the DC voltage evaluation of the BLDC motor same as the DC link voltage of the VSI. Connecting Four solar panels in series = 8 x 18.50 = 74 V

Total Power of Panel is 4 X 250 = 1000 W

An BLDC Motor of 816 Watts is selected for proposed system. The capacity of PV array should be equivalent to the motor. In this case a PV array is selected as of 1 KW.

$$P_{mmp} = (N_p \times I_{mpp}) \times (N_s \times V_{mpp}) = 1 \text{ Kw}$$

Table 1: Data Used in the Photovoltaic (PV) Modeling

PV details	
Number of cells in Modules	72
Open circuit voltage	22.32
Short circuit current	14.50
Voltage at MPP, Vm	18.50
Current at MPP, Im	13.52
For a PV Array	
Voltage at MPP, Vmpp=Vpv	74 V
Current at MPP, Impp=Ipv	Pmpp/Vmpp=1000/74=13.5
Power at MPP, Pmpp=Ppv	1000 W
Number of modules in Series Ns	Vmpp/Vm=74/18.50=4
Number of Modules in Parallel Np	Impp/Im=13.50/13.50=1

Where Pmpp is the maximum power that can be drawn from panels at a given radiation, Vmpp is the PV panel voltage at maximum power point and Impp is the current at maximum power point, Ns and Np are the number of panels related in series and parallel, respectively. The individual modules and array specifications are provided in table I.

Output voltage of panel = 74; Ppv = 1000 watts; Impp = 13.50 amps; Vmpp = 74

$$I_{mpp} = i_{pv} = \frac{P_{pv}}{V_{pv}} = \frac{1000}{74} = 13.50 \text{ Amps}$$

$$N_s = \frac{V_{mpp}}{V_m} = \frac{74}{18.50} = 4$$

$$N_p = \frac{I_{mpp}}{I_m} = \frac{13.52}{13.52} = 1$$

i. P&O MPPT algorithm

The Perturb and Observe based MPPT controller used in the proposed system is fed with voltage and current determined from the photovoltaic panel output, which is managed to produce the value of obligation at which the maximum power from the photovoltaic will be available. This task is nourished by a PWM creator where the production of pulses to the converter gates at the condenser terminals between photovoltaic and DC-DC converter is in comparison with a repeated categorization. Maximum power extraction and, subsequently, performance optimization of the SPV system is achieved. The Fig.3 shows a detailed flowchart.

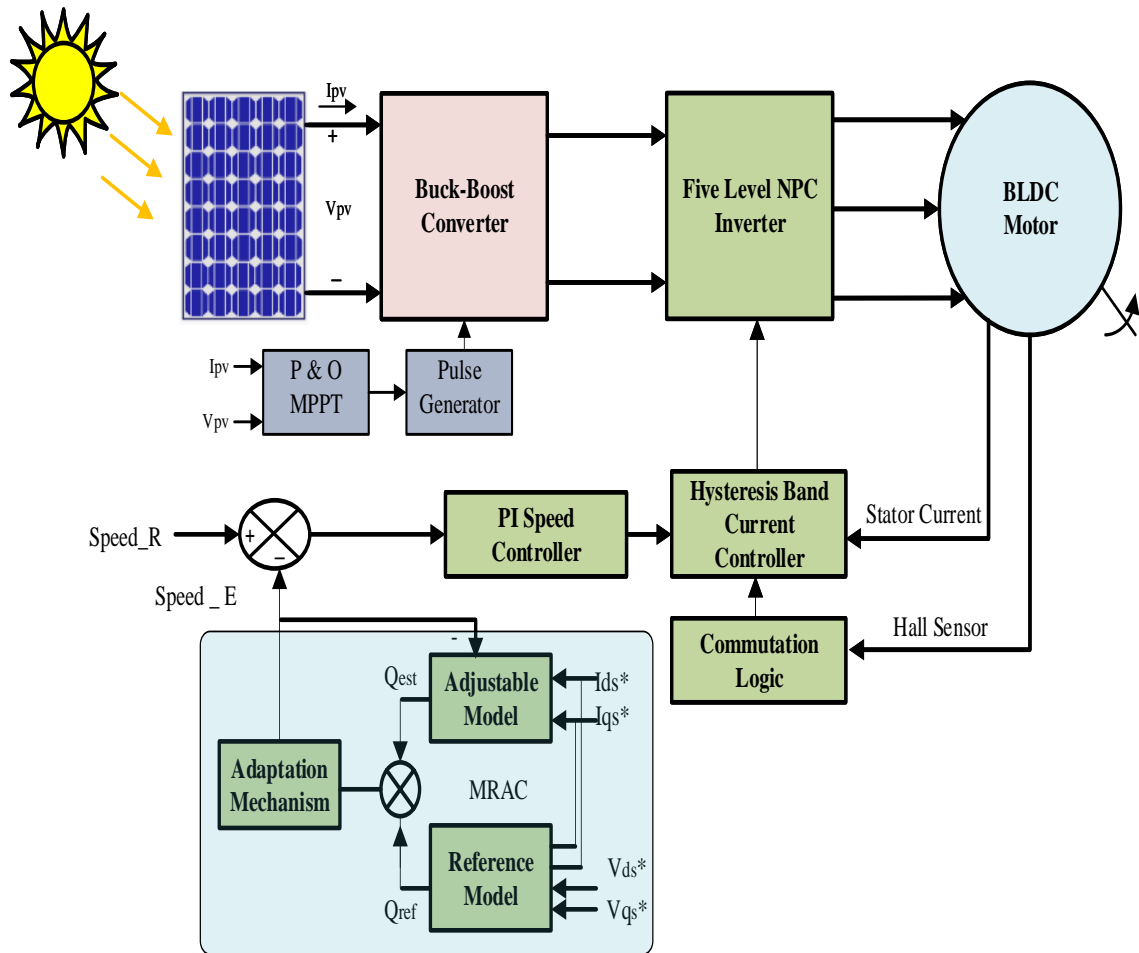


Figure 1: Proposed Methodology of Block Diagram

ii. Front End Converter (Buck Boost)

The Proposed buck boost converter fed BLDC motor drive which operates on continuous current mode. The principle of operation of the converter constituted in the three mode.

1. Mode I: The switch is ON and ON and the diode is OFF if the switch is ON and the diode is reversed biased and the current passes via the input inductor. The current of the input inductor increases and the energy is retained to the maximum extent possible, subject to applied voltage throughout the inductor.
2. Mode II: Switch is OFF and Diode is ON condition. When is switch is OFF state effective energy stowed in the input inductor is discharged to dc link capacitor. The input inductor current decreases to zero and dc link capacitor remains on a charge state.
3. Mode III. Switch OFF and Diode is OFF. When switch and diode is are in OFF Condition and dc link capacitor discharges the energy is fed to the load.

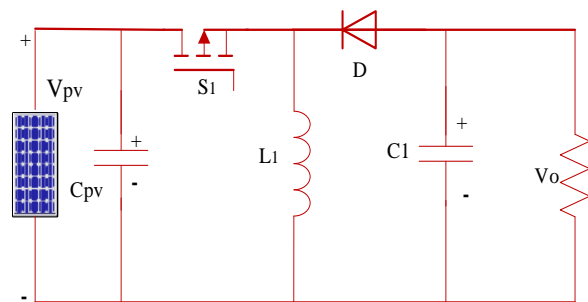


Figure 5: Solar fed Buck-Boost Converter

The photo voltaic array generates the power as shown in Fig.5, and feeds the buck-boost converter. The buck-boost converter's semiconductor switch is operated through a Perturb and Observe (P&O), maximum Power Point Tracking techniques such that the solar array cycle is enhanced and the BLDC motor has a gentle start. Typically, the converter is operated in continuous conduction mode to reduce stress on the issues and semiconductor devices.

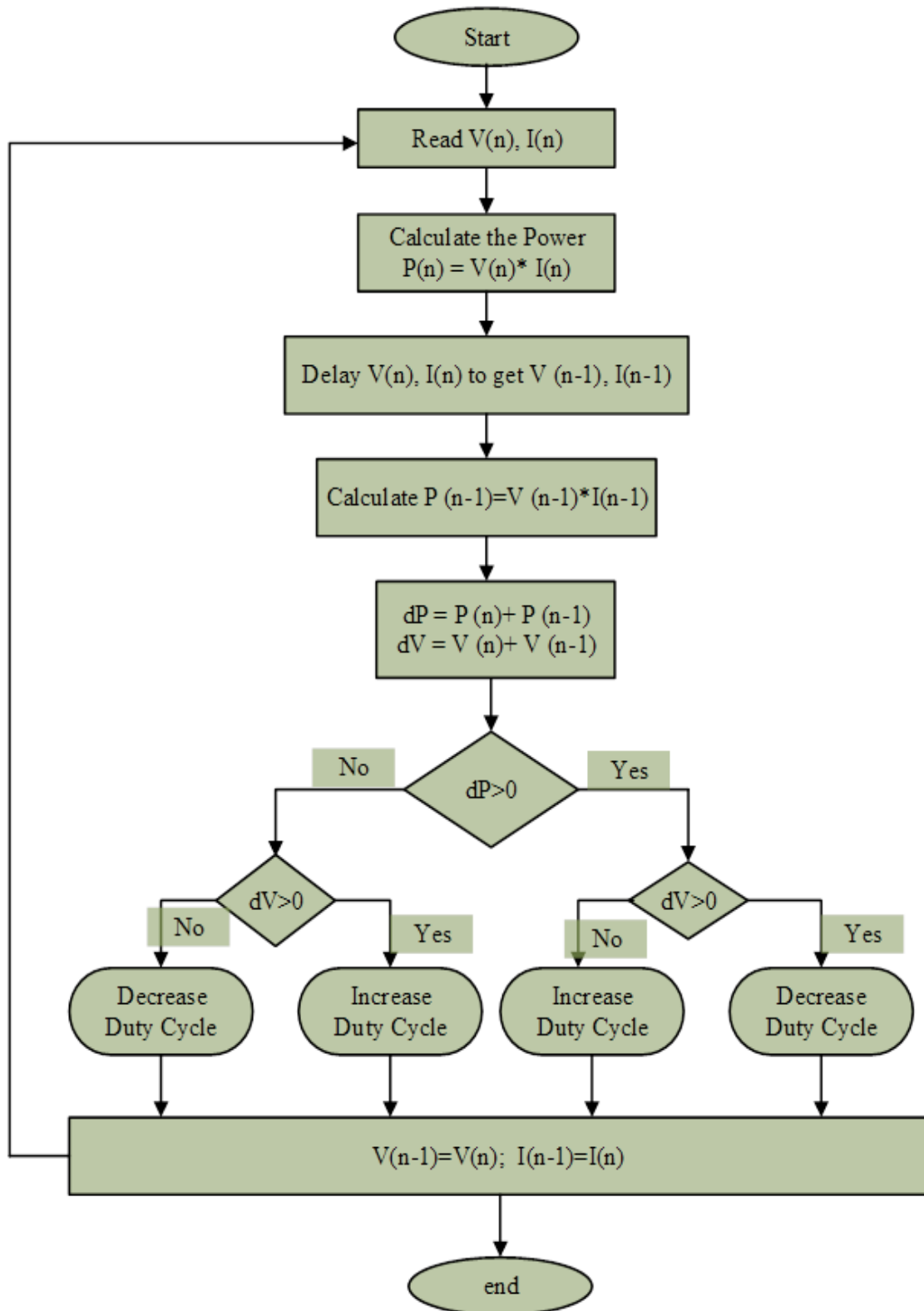


Figure 3: Detailed P & O flowchart

Switching categorization for the Voltage Source Inverter is given with the aid of Brushless motor's electronics commutation. Electronic commutation is a technique of decoding the Hall Effect indicators produced

by the motor built-in encoder in accordance with the rotor's position. In the resulting sectors the configuration and manipulation of the proposed gadget is specified.

The voltaic picture array voltage at MPP, $v_{pv} = V_{mpp} = 74$ V appears as the input voltage supply but the voltage DC of the voltage source, v_{dc} appears as the converter's output voltage. The buck-boost converter's obligation duty ratio, D is rated, the input-output consumption.

$$D = \frac{V_{dc}}{V_{dc} + V_{pv}} = \frac{250}{250 + 74} = 0.7716$$

Relationship as

Where $V_{dc} = 250$ V is calculated to be the DC voltage of the voltage source and I_{dc} the average current.

$$I_{dc} = \frac{P_{mpp}}{V_{dc}} = \frac{1000}{250} = 4 \text{ Amps}$$

4. Proposed Multilevel Inverter (NPC) Topology Fed BLDC

Illustration. 1 Displays the proposed converter configuration consisting of a five-level NPC inverter to reduce the current ripple, a Buck-Boost converter to change the DC voltage, and a switching voltage determination circuit to apply the desired switching voltage at the start of the switching cycle. The five-level NPC inverter used by MOSFET operates at a switching frequency of 80 kHz and achieves better overall efficiency at the same switching frequency than the three-level fundamental inverter[12]. The voltage stress throughout the MOSFET-diode module is half the normal inverter's DC voltage, which very expressively eliminates switching and conduction losses. The C1 and C2 condensers are operating on separating the DC voltage, which defines the neutral point.

The clamping diodes are used to transversely limit the voltage of the condensers to half the dc bus voltage. The direction of the commutation interval of five-level MLI leg A. The resulting modes of action of the 5-level NPC inverter are discussed primarily on the basis of the voltage polarity in the direction of the charge current and the inverter terminals.

The topologies used most commonly are neutral-point-clamped (NPC). In the clamped inverter neutral-point, the dc-link is dc link is section into many ranges of littler voltage stages using mass capacitors connected with an association bank. The inverter assembly enables one of these voltage levels to be attached to the inverter shafts, thereby producing an impressive voltage waveform at the device. Figure 1 looks at a three-phase, five-level diode-clipped inverter. Each three phases of the inverter portions a common dc bus, which is again subdivided into six levels by means of four condensers[1].

The voltage is V_{dc} throughout each capacitor, and the voltage tension is very much limited to V_{dc} through the clamping diodes throughout each switching process. Changing prerequisites for the 5 level NPC inverter are shown in Table1. State situation 1 The turn is on, and the exchange is off 0 techniques. Every stage has 5 respective

swap sets. The crucial stage leg turn units and are (Sa1, Sa1), (Sa2, Sa2), (Sa3, Sa3) and (Sa4, Sa4)[2]. Table also shows that the switches on for a specific stage leg are continuously connected and in arrangement in a diode clipped inverter.

Table 1: State switching table of Five level inverter

Switching States								Output Voltage
Sa1	Sa2	Sa3	Sa4	Sa5	Sa6	Sa7	Sa8	
0	0	0	1	1	1	0	0	-2Vo
0	0	0	1	1	0	0	1	-Vo
0	0	0	1	0	0	1	1	0
0	0	1	0	0	0	0	0	0
0	1	1	0	0	0	1	0	-2Vo
1	1	1	0	0	0	0	0	Vo

The benefits of NPC inverter are that the whole stages portion a typical dc bus voltage, which limits the capacitance necessities of the inverter. Hence, a consecutive topology isn't just conceivable yet in addition reasonable for utilizations, for example, a Consecutive high-voltage between link or adjustable speed drive. As a meeting the condensers can be resurrected. Proficiency is high for key recurrence exchanging.

The hall sensor output stretches out the rotor position data. True speed is calculated by measuring the imitation of the position of the rotor and finishing a low pass filter by passing it. A speed regulator which in this case is of proportional integral category is given the error produced by comparing the real and the reference speeds. This device approaches the wave signal of error to create a reference torque signal. The reference torque is converted to contemporary reference signal that is important for reference currents in the period.

The cutting-edge computing block takes the input from the output of the Hall sensor, produces the reference currents which are then equated with the real i_a^* and i_b^* currents, and produces error alerts which are then treated via a current controller (PI) and Sa, Sb and Sc reference signals are controlled. These indicators are fed in on the inverter to the PWM module. This block ensures function of a reference signal model. Such modulating warnings are provided by a triangular wave with a carrier frequency of $f_c = 80$ kHz to produce PWM pulses for the inverter. The pressure is applied in MATLAB Simulink, using the Sim Power library.

a. MRAS based BLDC Motor Drives

The model adaptive reference system (MRAS) looks like one of the many capable methods that function in adaptive control for a wide variety of applications. This owes to the fact that a proportion of the difference between the reference model's outputs and the adjustable

model can be obtained without delay by comparing the reference model's states (or outputs) with those in the adjustable system.

An Adaptive controller covers a lot of procedures which give a precise way to deal with programmed modification of controllers progressively, so as to accomplish or to keep up an ideal degree of control framework execution when the parameters of plant dynamic model might be obscure/or change in time.

However, when the plant parameters either remain unknown or change in time, it augurs an adaptive approach in order to achieve and maintain the desired performance using a reference model.

The strategy explained in Figure 4 details the structure with a control method using the dq frame for the control of both the current and speed through the theory of MRAC. The stator current sensed from the dq frame and converted to speed signal calculates the error which when amplified and compared with triangular carrier wave enables the generation of the PWM pulses for the NPC inverter switches.

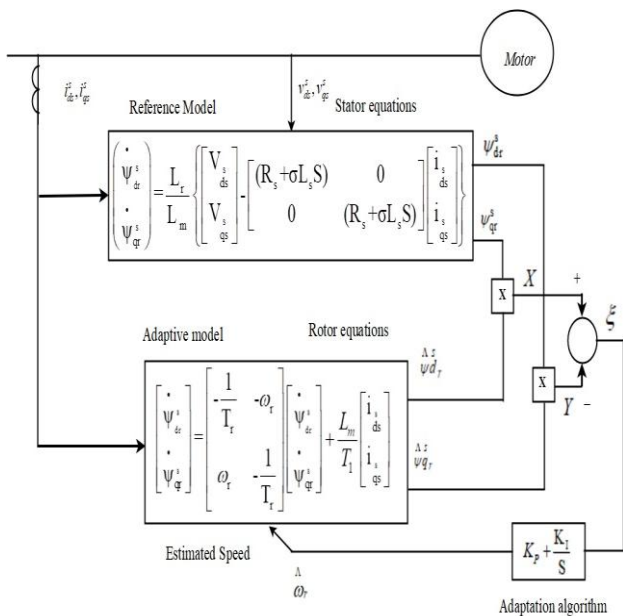


Figure 4: Diagram of MRAC fed BLDC Motor

Figure 5 represents the MRAC's use in solving the technique for speed estimation. The speed predictable by the back EMF and the speed intended by the Hall sensors form the inputs of the regulator. The output of the regulator relates to the corrected variable for the estimated speed.

Our aim is to solve these two problems noted above, one time a speed estimation algorithm was planned based primarily on MRAC. Diagram. 4 Indicates the main diagram of the speed governor method with the algorithm suggested for the speed estimation. This consists of a control and power circuit that performs successive roles: speed and current regulation, technique PWM, control of speed estimation. The prevailing speed estimation blocks

are a regulator based on the MRACs. The controller's inputs are the speed determined by the EMF level and back measured with the help of Hall sensors. The regulator output is a correction vector to the projected speed.

The approximate velocity is Spd_E. Spd_S is the velocity determined via Hall sensors. When Spd_E is no longer equivalent to Spd_S, a correction will be made through the PI regulator and then Spd_E will again be determined based entirely on the model proposed. With the assistance of the speed controller the reference current iref is modified. The inverter's output voltage is tuned via the current controller, and Spd_S is modified. In this way, the PI regulator used in the Procedure estimation still operates until Spd_E is equal to Spd_S.

b. Speed Estimation Algorithm

The error of calculating low speed is mostly directly dependent on the voltage of the stator resistor. So, firstly, an estimation method compensation of stator resistor voltage is provided. It shows up in Fig. 5. In Rs the temperature is not currently right or changed, Spd E will no longer be equal to Spd S. Because kc influences Spd E and PI controller speed, the controller adaptively compensates the output voltage to the stator resistor's divided voltage. Continually tunes kc when the actual speed and reference are equal. This proposed algorithm can therefore keep the approximate precision very small.

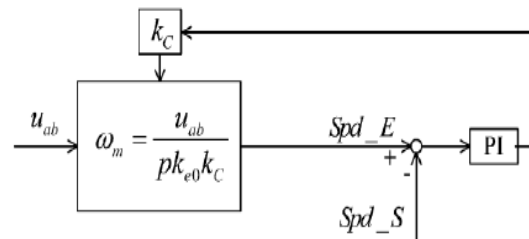


Figure 5: low speed turned PI controller

5. Simulation Results

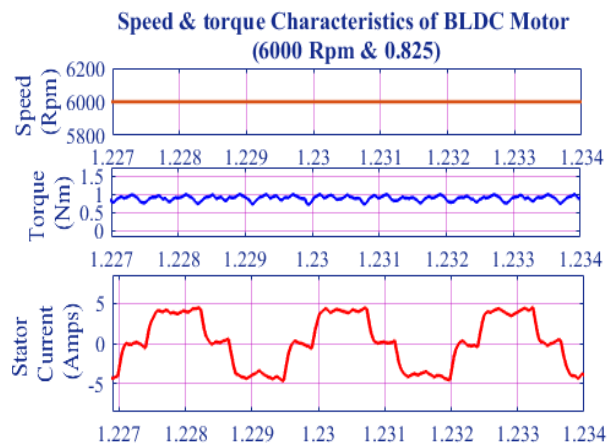


Figure 6: Speed & Torque Characteristics of BLDC motor

In this figure show that motor speed 6000 rpm and torque 0.825 Nm.

Illustration. 6 Specifies the simulation results obtained for a reference speed of 6000 rpm when it reaches at 0.1 s. The current and speed waveforms are obtained for condition of no load and full load. The optimum DC voltage is i. e. To furnish the appraised motor speed to 250V. The answer is speed and current is very strong. In any case, the stock to the motor should be multiplied for above base speed and requirements for a growth in the DC voltage that is incredible if a PWM achieved inverter continued BLDC drive has to occur.

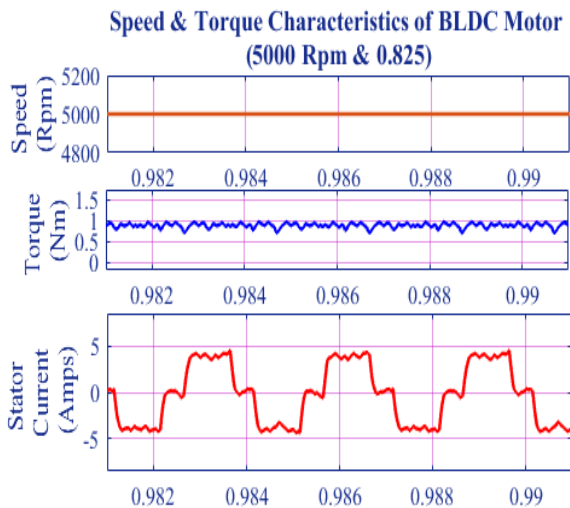


Figure 7: Speed & Torque Characteristics

In this figure show that motor speed 5000 rpm and torque 0.825 Nm.

Illustration. 7 Displays the speed response, phase 'a' stator current response and torque response of the 5000-rpm motor at load of 0.825 Nm torque its reaches at 0.1 sec. The speed response is good and minimized torque ripples.

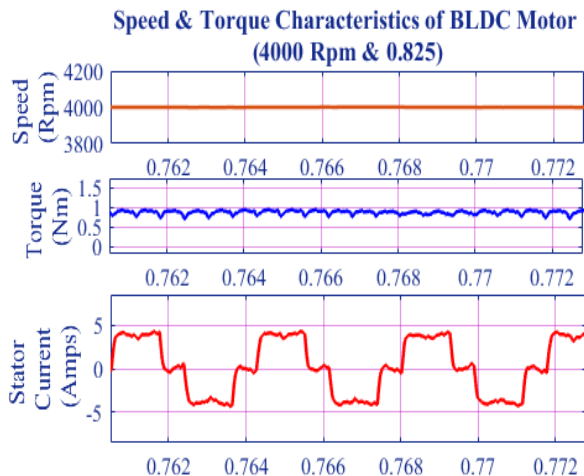


Figure 8: Speed & Torque Characteristics

In this figure show that motor speed 4000 rpm and torque 0.825 Nm.

Fig. 8 shows the response for 4000 rpm at load of 0.825 Nm, applied at 0.1 sec. In this buck boost converter fed BLDC Motor reaches minimum torque ripple and low THD.

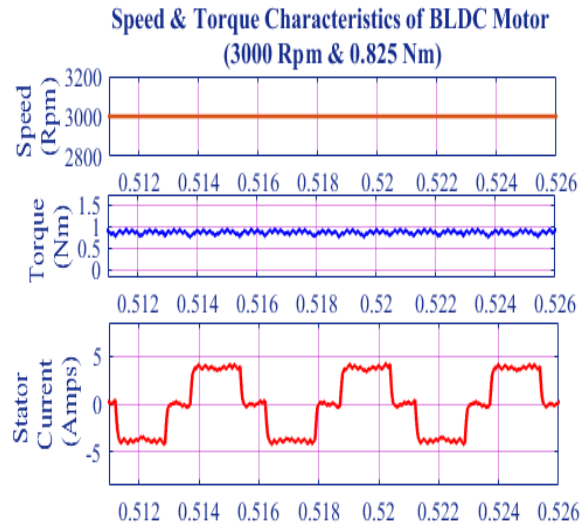


Figure 9: Speed & Torque Characteristics

In this figure show that motor speed 3000 rpm and torque 0.825 Nm.

Illustration. 9 Displays the speed response, the phase 'a' stator current response and the torque response of the 3000 rpm motor at a load of 0.825 Nm of torque applied at 0.1 sec. The ripple of the stator current is very low so that THD is weak too. So good performance with BLDC motor.

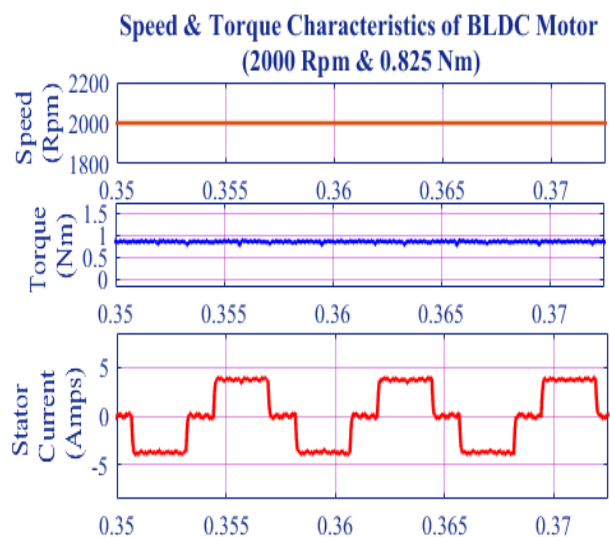


Figure 10: Speed & Torque Characteristics

In this figure show that motor speed 2000 rpm and torque 0.825 Nm.

Illustration. 10 Displays the speed response, the phase 'a' stator current response and the torque response of the 2000 rpm motor at a load of 0.825 Nm of torque applied at 0.1 sec. The ripple of the stator current is very low so that THD is weak too. So good performance with BLDC motor.

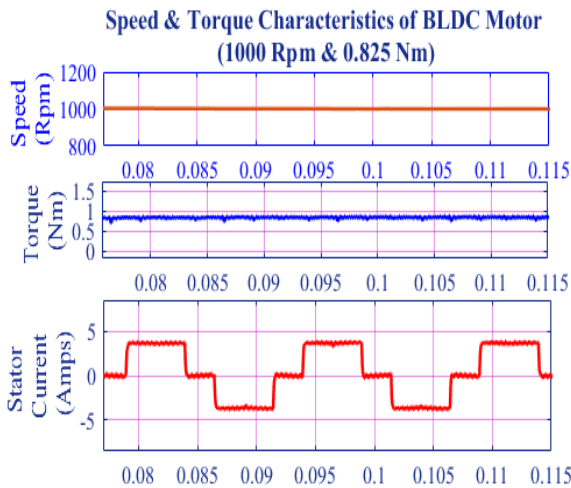


Figure 11: Speed & Torque Characteristics

In this figure show that motor speed 1000 rpm and torque 0.825 Nm.

Illustration. 11 Displays the speed response, the phase 'a' stator current response and the torque response of the 1000 rpm motor at a load of 0.825 Nm of torque applied at 0.1 sec. The ripple of the stator current is very low so that THD is weak too. So good performance with BLDC motor.

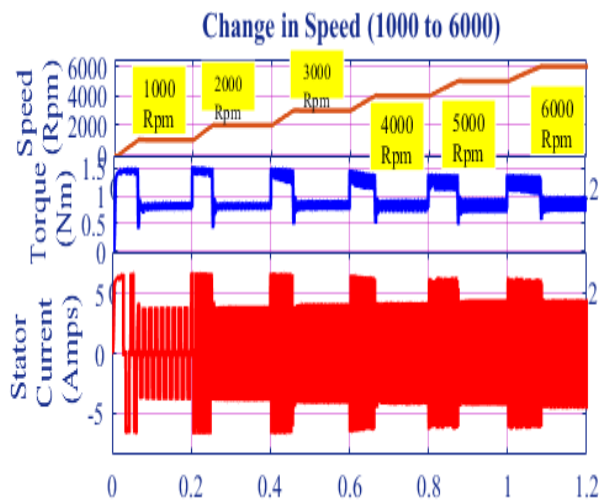


Figure 12: Change in Speed Characteristics

In this figure show that change in motor speed 1000 to 6000 rpm and torque 0.825 Nm.

Illustration. 12 Displays the speed, phase 'a' current and torque response engine for the reference full load of 0.825 Nm torque applied at each 0.2 sec and the velocity

of 1000 to 6000. The speed setting of 1000 rpm torque will increase but finally set 0.825 for every shift in response speed. When beginning, the torque value reaches 1.5 Nm, and then set the usual torque.

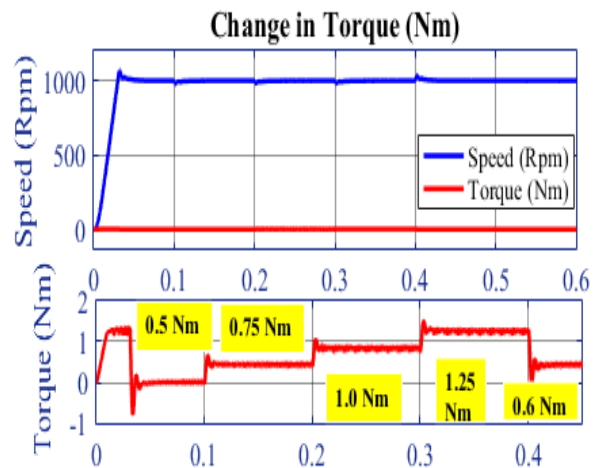


Figure 13: Change in Load (Torque Nm) Characteristics

In this figure show that change in motor Load 0.5 Nm to 1.25 Nm and reference speed 1000 Rpm.

Illustration. 13 Displays the speed, phase 'a' current and torque response motor for the reference full load of 1000 rpm speed applied at each 0.2 sec and the torque of 0.5 Nm to 1.25Nm. The torque setting of 0.5 Nm speed will increase but finally set 1000 Rpm for every shift in response speed. When beginning, the speed value reaches 1005 Nm, and then set the usual speed (1000 Rpm).

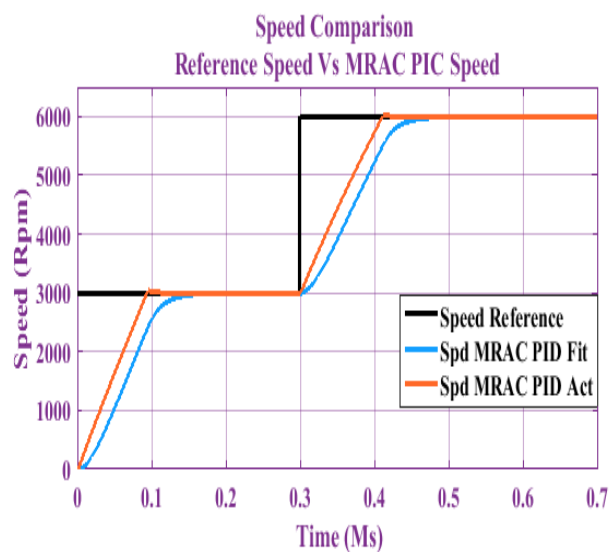


Figure 14: Speed Characteristics with MRAC

In the figure 14 show that various speed characteristics BLDC, black indicate reference speed and blue and orange indicate MRAC_PID act and fit. Its clearly indicate MRAC speed is better than other controller performance.

Table 3: Performance analysis of different load conditions

S. No	Load Torque (N-m)	Inverter Voltage THD	Stator Current THD	Speed (RPM)	Setting Time (ms)
1.	0.5	4.785	3.672	1500	0.1
2.	1.0	4.265	2.980	1500	0.12
3.	1.5	3.568	2.238	1500	0.15
4.	2.0	3.127	1.851	1496	0.18
5.	2.5	2.205	1.265	1490	0.20

Table 3 shows the variations in the load (Nm) with inverter THD, stator current THD and Reference Speed 1500 Rpm. Increase the load (Nm) low value of THD in all condition.

S. No	Parameter	Values
1	Rated Voltages (V)	250
2	Phase Inductance (mH)	3.09
3	Phase Resistance (Ω)	3.10
4	Back Emf (V/(rad/s))	0.227
5	Rated Torque (Nm)	0.825
6	Rated Speed (Rpm)	6000
7	Rated Power (W)	816
8	Pole Pairs	4

6. Conclusion

Sun energy condition based five-level inverter which uses associated with brushless engine which is utilized as burden. The curios of a MRAC have been looked to permit a shut activity. The simulation was done utilizing MATLAB Sim power system. Taking the benefits of generally excellent change effectiveness of buck-boost converter, the BLDC engine. The proposed framework is structured splendidly, with the end goal that the presentation isn't influenced by the climate condition and proficiency confinements of the converters and engines. The Total harmonic distortion of output current and voltage of the five level inverter has diminished and subsequently an expansion of the productivity of the engine will be accomplish lower estimations of the THD for the stator current and the inverter yield voltage guarantee an upgrade in power quality.

7. Acknowledgements

This publication is an outcome of the R&D work undertaken from the project under the Visvesvaraya Ph.D. Scheme of the Ministry of Electronics and Information Technology, Government of India, being implemented by Digital India Corporation. Implementation Order No. and Date: Ph.D-MLA/4(82)/2015-2016 dated 15.04.2016.

https://phd.medialabasia.in/student_info.php?institute=Annamalai%20Unversity,%20Tamil%20Nadu&f=&enrollment=Full%20Time.

References

- [1] M. Ouada, M.S. Meridjet and N. Talbi, "Optimization Photovoltaic Pumping System Based BLDC Using Fuzzy Logic MPPT Control," *International Renewable and Sustainable Energy Conference (IRSEC)*, pp. 27-31, 7-9 March 2013.
- [2] F.A.O. Aashoor and F.V.P. Robinson, "Maximum Power Point Tracking of Photovoltaic Water Pumping System Using Fuzzy Logic Controller," *48th International Universities' Power Engineering Conference (UPEC)*, pp.1-5, 2-5 Sept. 2013.
- [3] A.M. Noman, K.E. Addoweesh and H.M. Mashaly, "Simulation and dSPACE Hardware Implementation of the MPPT Techniques Using Buck Boost Converter," *AFRICON*, pp.1-9, 9-12 Sept. 2013.
- [4] B. Subudhi and R. Pradhan, "A Comparative Study on Maximum Power Point Tracking Techniques for Photovoltaic Power Systems," *Sustain. Energy, IEEE Trans.*, vol. 4, no. 1, pp. 89-98, 2013.
- [5] M. H. Taghvaei, M. A. M. Radzi, S. M. Moosavain, H. Hizam, and M. Hamiruce Marhaban, "A current and future study on non-isolated DC-DC converters for photovoltaic applications," *Renew. Sustain. Energy Rev.*, vol. 17, pp. 216-227, 2013.
- [6] M. Bertoluzzo, G. Buja, R. K. Keshri, R. Menis, "Sinusoidal Versus Square-Wave Current Supply of PM Brushless DC Drives: A Convenience Analysis", *IEEE Transactions On Industrial Electronics*, Vol. 62, No. 12, pp. 7339-7349, 2015.
- [7] Microsemi "Speed control of Brushless DC motors- Block Commutation with Hall sensors"
- [8] Rajan Kumar and Bhim Singh, "Solar PV Array Fed Cuk Converter-VSI Controlled BLDC Motor Drive for Water Pumping," *6th IEEE Power India International Conference*, pp. 1-7, Feb 2014.
- [9] Dhaval D. Julasana, Sagar B. Dabhi, Chirag H. Raval, "Simulation and Analysis of PMSBLDC Motor fed by Seven Level Inverter with K-map Logic", *International Conference on Computing, Power and Communication Technologies (GUCON) Galgotias University, Greater Noida, UP, India. Sep 28-29, 2018.*
- [10] B.Mahesh Babu, L.Ravi Srinivas, B.Bindhu, "A MLI Topology with Different Braking Mechanisms Employing BLDC Drive", *IEEE International Conference on Power, Control, Signals and Instrumentation Engineering (ICPCSI-2017)*.
- [11] Bonula Sowjanya Kalyani, Venu Madhav Mukkavilli, Dr. Gopichandnaik, "Performance Enhancement of Permanent magnet Brushless

- Dc Motor Using Multilevel Inverter”, IEEE 7th International Advance Computing Conference 2017.
- [12] Veeramuthulingam N, Ezhilarasi A & Ramaswamy M, “Steady State Performance Enhancement Strategy for Brushless DC Motor Drive using Model Reference Adaptive Control”, Journal of Advanced Research in Dynamical and Control Systems, Volume 07-Special Issue, pages 881-895, June 2018.
- [13] N. Veeramuthulingam, A. Ezhilarasi, M. Ramaswamy, P. Muthukumar, “Modeling of Brushless DC Motor Using Adaptive Control”, Soft Computing Systems. ICSCS 2018. Communications in Computer and Information Science, 837, pp. 764-775, 2018.
- [14] C. Gnanavel, T. Baldwin Immanuel, P. Muthukumar, Padma Suresh Lekshmi Kanthan, “Investigation on Four Quadrant Operation of BLDC MOTOR Using Spartan-6 FPGA”, Soft Computing Systems. ICSCS 2018. Communications in Computer and Information Science, 837, pp. 752-763, 2018.
- [15] KVNS Pavan Kumar, Dr.S.Prakash, “Modeling Simulation of BLDC Motor and HEV Motor System Using Adaptive Neuro Fuzzy (ANFIS) Inference Algorithm”, Test Engineering and Management, Volume 82, Pages: 2242 – 2249, Issue: January-February 2020.